An improved experimental pipeline for preparing circular ssDNA

viruses for next-generation sequencing

Catherine D. Aimone[1], J. Steen Hoyer[2], Anna E. Dye[1], David O. Deppong[1], Siobain Duffy[2],

Ignazio Carbone[3], Linda Hanley-Bowdoin[1*]

[1]Department of Plant and Microbial Biology, North Carolina State University, Raleigh NC
    27695 USA
[2]Department of Ecology, Evolution, and Natural Resources, Rutgers University, New
    Brunswick, NJ 08901USA
[3]Department of Entomology and Plant Pathology, North Carolina State University, Raleigh NC
    27695 USA

[*]Address correspondence to Catherine D. Aimone, cddoyle@ncsu.edu

15 Abstract

16 We present an optimized protocol for enhanced amplification and enrichment of viral DNA for

17 Next Generation Sequencing of begomovirus genomes. The rapid ability of these viruses to

18 evolve threatens many crops and underscores the importance of using next generation

19 sequencing efficiently to detect and understand the diversity of these viruses. We combined

20 enhanced rolling circle amplification (RCA) with EquiPhi29 polymerase and size selection to

21 generate a cost-effective, short-read sequencing method. This optimized protocol produced short-

22 read sequencing with at least 50% of the reads mapping to the viral reference genome. We

23 provide other insights into common misconceptions about RCA and lessons we have learned

24 from sequencing single-stranded DNA viruses. Our protocol can be used to examine viral DNA

25 as it moves through the entire pathosystem from host to vector, providing valuable information

26 for viral DNA population studies, and would likely work well with other CRESS DNA viruses.

Keywords: phi29, EquiPhi29, MiSeq, whiteflies, viral DNA sequencing

Highlights

- Protocol for short-read, high throughput sequencing of single-stranded DNA viruses using random primers

- Comparison of the sequencing of total DNA versus size-selected DNA

- Comparison of phi29 and Equiphi29 DNA polymerases for rolling circle amplification of viral single-stranded DNA genomes

27

28

1. Introduction

Begomoviruses, one of the nine genera in the *Geminiviridae*, are single-stranded DNA (ssDNA) viruses that infect a wide variety of plant species, including many important crops. They are also classified as CRESS DNA viruses, a large group of circular ssDNA viruses that encode replication-associated proteins (Rep) originating from a common ancestor (Zhao et al., 2019). Eukaryotic CRESS DNA viruses impact a wide range of plant and animal hosts and evolve rapidly (Zhao et al., 2019).

Cassava and tomato are among the important crops whose yields are severely impacted by begomovirus diseases. Cassava is an important root crop in Africa, Asia, and Latin America, with African farmers producing over half of the total cassava worldwide (FAOSTAT, 2016). In Africa and more recently in Asia, cassava yields have been reduced by Cassava mosaic disease (CMD), which is caused by a complex of 11 begomoviruses collectively referred to as cassava mosaic begomoviruses (CMBs). Annual cassava losses in Africa have been estimated to be 15-24% or 12-23 million tons (US $1.2-2.3 billion) (Thresh J. M. , 1997; Uzokwe et al., 2016). In some regions of Africa, cassava farmers have experienced losses of up to 95%. Tomato, an important vegetable crop that is grown around the world, is a host for over 100 begomovirus species, with the most devastating being tomato yellow leaf curl virus (Moriones and Navas-Castillo, 2000). In the eastern United States, tomato production is also negatively impacted by a second begomovirus, tomato mottle virus (ToMoV), which causes widespread disease with yield losses of up to 50% (Abouzid, Polston, and Hiebert, 1992; Polston and Anderson, 1997). Given their significant impact on agriculture, it is important to understand how begomoviruses change over time and adapt to new hosts and environments. Next generation sequencing (Jeske, 2018) is an important approach for gaining insight into begomovirus populations.

52   Begomoviruses fall into two classes – the Old World viruses and the New World viruses

53   (Lefeuvre et al., 2011). Their genomes consist of either one or two circular DNAs. CMBs are

54   Old World viruses, while ToMoV is a New World virus. The genomes of the CMBs and ToMoV

55   consist of two components designated as DNA-A and DNA-B that together total 5-6 Kb in size.

56   Both components are required for systemic infection (Stanley and Gay, 1983). The genome

57   components contain divergent transcription units separated by a 5' intergenic sequence that

58   contains the origin of replication and promoters for gene transcription (Hanley-Bowdoin et al.,

59   2013). DNA-A encodes 5-6 proteins necessary for replication, transcription, encapsidation, and

60   combatting host defenses (Hanley-Bowdoin et al., 2013). DNA-B encodes two proteins essential

61   for movement (Hanley-Bowdoin et al., 2013).

62   Begomoviruses are encapsidated into double icosahedral virions and transmitted by

63   whiteflies (*Bemisia tabaci*) (Hanley-Bowdoin et al., 2013). When a whitefly feeds on the phloem

64   of an infected plant, it acquires virions that can be transmitted to a healthy plant during the next

65   feeding cycle. Structural studies have shown that a begomovirus virion only contains one ssDNA

66   molecule, such that the DNA-A and DNA-B components of bipartite viruses are packaged

67   separately into virions (Bottcher et al., 2004). As a consequence, successful transmission of a

68   bipartite begomovirus requires acquisition and transmission of at least two virions – one

69   containing DNA-A and another containing DNA-B. Once the virions enter a phloem-associated

70   cell, viral ssDNA is released, converted to double-stranded DNA (dsDNA), and replicated via a

71   rolling circle mechanism (Hanley-Bowdoin et al., 2013). As infection proceeds, nascent viral

72   ssDNA can undergo multiple rounds of replication or be packaged into virions for future

73   transmission by whiteflies. ToMoV is only transmitted by whiteflies, while CMBs can be

74   transmitted via vegetative propagation of infected stem cuttings as well as by whiteflies (Legg et

75   al., 2014).

76   Begomoviruses have been shown to evolve rapidly (Duffy and Holmes, 2009; Lima et al.,

77   2017; Rocha et al., 2013), making them good models for studying the evolution of ssDNA

78   viruses. Many factors can contribute to begomovirus evolution, including agricultural practices,

79   whitefly transmission, and abiotic stress. This underscores the importance of understanding how

80   begomoviruses evolve through an entire pathosystem from host to vector. Generally, ssDNA

81   viruses exist as genetically diverse populations, with variation similar to that of RNA virus

82   populations (Elena and Sanjuán, 2007; Safari and Roossinck, 2014). The high genetic diversity

83   of virus populations is linked to their rapid ability to evolve, to emerge in a new host, and to

84   break disease resistance (Duffy, 2008). Viral diversity is driven by high mutation and

85   recombination rates (Lefeuvre and Moriones, 2015; Sanjuán et al., 2010). The amount and type

86   of genetic variation within a viral population is a direct measure of evolvability and pathogenesis

87   (de la Iglesia and Elena, 2007; Elena, Fraile, and García-Arenal, 2014; Elena and Sanjuán, 2007).

88   However, our ability to study viral evolution in real-time has been limited by being able to

89   accurately describe the genetic structure of viral populations over time (Acevedo, Brodsky, and

90   Andino, 2014).

91   Deep sequencing technologies have advanced our understanding of the genetic variation

92   of evolving virus populations, beyond virus identification and characterization of viral species

93   (Acevedo et al., 2014). Next generation sequencing can provide insight into how viral

94   populations, as quasi-species, are highly variable with a range of beneficial or neutral mutations

95   that occur at low frequency (Dean et al.; Dickins and Nekrutenko, 2009). With NGS, we can

96   actively track naturally occurring viral variants through infection, adaptation to new hosts, and

97   host range expansion (Ruark-Seward et al., 2020). Yet, the ability of NGS to track viral variants

98   is restricted by several technical challenges, including biased amplification, errors introduced

99   during amplification and sequencing, and low viral read depth.

100   Current methods of viral amplification rely on the polymerase chain reaction (PCR) using

101   virus-specific primers and Taq polymerase or rolling circle amplification (RCA) using random

102   hexamers and phi29 DNA polymerase (Dean et al., 2001). Unlike RCA, sequence-specific PCR

103   can introduce sequence bias that masks viral diversity in a population (Sipos et al., 2010). RCA

104   amplifies circular episomes like begomovirus genomes more efficiently than linear DNA,

105   thereby enriching for begomovirus sequences (Idris et al., 2014). RCA is less susceptible to

106   sequence bias, less error-prone than traditional PCR, and does not fix errors in the sample to be

107   sequenced (Lou et al., 2013; Wang et al., 2014). However, RCA produces hyper-branched,

108   concatenated products (Lasken and Stockwell, 2007), that must be linearized by restriction

109   enzyme digestion or mechanical shearing before NGS sequencing (Inoue-Nagata et al., 2004).

110   Short-read sequencing in combination with RCA and size selection has improved viral read

111   depth for RNA viruses (Acevedo and Andino, 2014; Acevedo et al., 2014). For DNA viruses,

112   long-read sequencing of size-enriched viral DNA has been successful in reducing sequencing

113   error (Mehta et al., 2019).

114   Short-read sequencing has been used in combination with RCA to enrich for CMB viral

115   sequences in cassava (Kathurima, 2016) and *Nicotiana benthamiana* (Chen, Khatabi, and

116   Fondong, 2019). Other begomoviruses species, including tomato leaf, curl New Delhi virus

117   (Juárez et al., 2019) and euphorbia yellow mosaic virus (Richter et al., 2016) have also been

118   amplified by RCA for short-read sequencing. Likewise, RCA has been used to improve read

119   depth of mastreviruses, which constitute another genus in the *Geminiviridae* (Claverie et al.,

120   2019). Depending on the research question, the methods cited above can return sufficient viral

121   read depth for identifying new viruses and determining the prominent viruses in an infected

122   plant. However, to reliably detect subconsensus viral variants in a population, a higher level of

123   coverage is required (Juárez et al., 2019).

124   Here, we describe an experimental pipeline for analyzing begomovirus DNA population

125   dynamics across a complete pathosystem constituted by the plant host and the insect vector. The

126   pipeline combines size selection and linear amplification by an improved phi29 DNA

127   polymerase to increase viral read coverage for diversity studies (Fig. 1).

128   **2. Methods**

129   *2. 1. Virus-infected plants and viruliferous whiteflies*

130   Cassava plants (*Manihot esculenta* cv. Kibandameno or Kibaha) were propagated from

131   stem cuttings and grown at 28°C under a 12-h light/dark cycle. Plants with ca. 8-10 nodes and

132   stems 1.5 cm in diameter (ca. 2 months after propagation) were inoculated at the apical meristem

133   using a hand-held micro sprayer (40 psi) to deliver gold particles coated with plasmid DNA (100

134   ng/plasmid/plant) (Ariyo et al., 2006; Cabrera-Ponce et al., 1997). The plasmids, which

135   contained partial tandem dimers of DNA-A and or DNA-B of *African cassava mosaic virus*

136   (ACMV; GenBank accessions MT858793.1 and MT858794.1) and *East African cassava mosaic*

137   *Cameroon virus* (EACMCV; AF112354.1 and FJ826890.1)(Chowda Reddy et al., 2012;

138   Fondong and Chen, 2011; Fondong et al., 2000; Hoyer et al., 2020). Three plants were co-

139   inoculated with both ACMV and EACMCV. Leaf punches from symptomatic cassava plants

140   were sampled at 28 days post-infection (dpi), flash-frozen in liquid nitrogen, and stored for

141   analysis.

142   Tomato seedlings (*Solanum lycopersicum* cv. Florida Lanai) were grown from seed at

143   25ºC under a 12-h light/dark cycle. Plants with five true leaves (ca. 4 weeks old) were

144   agroinoculated with ToMoV DNA-A and DNA-B (Abouzid et al., 1992; Reyes et al., 2013) as

145   described by Rajabu et al. (2018). An infected plant was sampled at the third leaf below the

146   apical meristem at 21 dpi, immediately prior to the whitefly access period for the acquisition of

147   ToMoV. The leaf tissue (1 mg) was separated into two parts, one part for total DNA extraction

148   and the other part for virion extraction. *Bemisia tabaci* MEAM1 adult whiteflies between 2 and

149   10 days post-eclosion were allowed to acquire the virus by feeding on a symptomatic plant

150   infected with ToMoV for an Inoculation Access Period (IAP) of 72 h (Ng et al., 2011; Rajabu et

151   al., 2018). Whiteflies were collected via aspiration and stored in 70% ethanol for analysis.

152   2.2 *DNA extraction and size selection*

153   Frozen leaf tissue was ground using a homogenizer (Model# MM 301, RETSCH-

154   Laboratory Mills, Clifton, NJ), and total DNA was extracted from leaf samples using the

155   MagMax^{TM} Plant DNA Isolation Kit according to manufacturer's instructions (Thermo Fisher

156   Scientific, Waltham, MA). Total DNA was extracted from groups of five whiteflies using the

157   Qiagen DNeasy Blood and Tissue kit according to the manufacturer's instructions (Qiagen,

158   Hilden, Germany). Total DNA from cassava, tomato, and whiteflies (250 ng) was size selected

159   for 1-6 Kb DNA on a 0.75% agarose gel at 25V DC for 3-8 h using the Blue Pippin Prep system

160   (Model # BDQ3010, Sage Science, Beverly MA). The amount of size-selected output DNA was

161   typically less than 1 ng.

162   Virion DNA was generated by homogenizing five whiteflies or resuspending 1 mg of

163   frozen cassava or tomato leaf tissue in 50 mM Tris, 10 mM $MgSO_4$, 0.1 M NaCl, pH 7.5,

164   followed by low-speed centrifugation. The supernatant was subjected to 0.22 µM filtration

165 followed by DNase I digestion (2.5 U for 3 h at 37°C). Virion DNA was isolated using the

166 QIAamp MinElute Virus Spin Kit (Qiagen, Hilden, Germany)(Ndunguru et al., 2016; Ng et al.,

167 2011; Rosario et al., 2015).

168 *2.3. Viral levels*

169 The concentration of ACMV DNA-A (primer pair - P3P-AA2F and P3P-AA2R+4R;

170 Table 1), DNA-B (primer pair - ACMVBdiv4 and ACMVBfor1; Table 1), and EACMCV DNA-

171 A (primer pair – EACMVQ1 and EACMVQ; Table 1) and DNA-B (primer pair –

172 EACMVBREV4 and EACMVBfor1.2; Table 1) were measured by quantitative PCR (qPCR) in

173 total DNA samples (0.01 μg) extracted from cassava leaf tissue and analyzed in 96-well plates

174 on a Max3000P System (Stratagene, San Diego CA). Primers were tested in conventional PCR to

175 optimize annealing temperature and amplification efficiency for qPCR. For ACMV DNA-A,

176 qPCR was performed using Power SYBR Green PCR Master Mix (Applied Biosystems, Foster

177 City CA), starting with a 2 min denaturing step at 94°C, followed by 30 cycles consisting of 15

178 sec at 94°C, 1 min at 60°C, 30 sec at 72°C. The PCR conditions for EACMCV DNA-A were 10

179 min at 95°C, followed by 30 cycles of 30 sec at 95°C, 30 sec at 60°C, and 30 sec at 72°C.

180 Reactions were performed in three technical replicates. ACMV DNA-B and EACMCV DNA-B

181 were run following the above conditions respectively with an annealing temperature of 58°C.

182 Viral DNA was quantified using a qPCR standard curve generated by amplification of a 10-fold

183 dilution series (10^{-10} to 10^{-16} g/μL) of plasmid DNA with a single copy of ACMV DNA-A or

184 EACMCV DNA-A following the protocol described by Rajabu et al. (2018). The concentration

185 of the template DNA in the reaction mix was converted from ng/μL to copy number/μL using the

186 following formula; $(C \times 10^{-9}/MW) \times NA$ where C = template concentration ng/μL,

187 MW = template molecular weight in Daltons, and NA = Avogadro's constant 6.022×10^{23}. MW

188 was obtained by multiplying the number of base pairs of a plasmid by the average molecular

189 mass of one base pair (660 g/mol). A base 10 logarithmic graph of copy number versus the

190 threshold cycle (Li et al., 2009) for the dilution factor was plotted and used as a standard curve to

191 determine the amount of viral DNA (copy number/µL) of total DNA in a reaction mix (Rajabu et

192 al., 2018).

193 The concentration of ToMoV genomic components was quantified by qPCR in total

194 DNA samples (0.01 µg) from tomato leaf tissue and in whiteflies (2 ng) using the DNA-A primer

195 pair, ToMoVA6-F, and ToMoVA6-R, and the DNA-B primer pair, ToMoVB4-F, and

196 ToMoVB4-R (Table 1). The qPCR protocol was the same as described above for ACMV with an

197 annealing temperature of 57°C for 1 min. Viral DNA was quantified using a qPCR standard

198 curve generated by amplification of plasmid DNA with a single copy of each ToMoV segment

199 (pNSB1691 and pNSB1692) following the method described above.

200 *2.4. Rolling circle amplification*

201 Total DNA (100 ng) from symptomatic Kibaha leaf tissue was amplified using the

202 TempliPhi Amplification Kit (GE Healthcare, Chicago IL), which contains phi29 DNA

203 polymerase (Dean et al., 2002), according to the manufacturer's instruction at 30°C for 18 h. The

204 reaction buffer solution of the TempliPhi Amplification Kit included random hexamer primers.

205 Separately, 2 µL of total DNA was denatured at 95°C for 3 min, then cooled on ice for 3 min for

206 amplification with the EquiPhi29 kit (Thermo Fisher Scientific, Waltham MA). The cooled

207 reaction was mixed with 0.5 µL of 10X EquiPhi29 Reaction Buffer, 1.0 µL of Exo-resistant

208 random primers, and 1.5 µL of nuclease-free water. The denatured DNA product (5 µL) was

209 amplified using 1 µL (10 U) of EquiPhi29 DNA polymerase, 1.5 µL of 10X EquiPhi29 Reaction

210 Buffer, 0.2 µL of 100 mM DTT, 2 µL of 10 mM dNTP mix, 1.0 µL (0.1 U) of pyrophosphatase

211   and 9.3 μL of nuclease-free water (Povilaitis et al., 2016) according to the manufacturer's

212   instructions, except that the reactions were performed at 40°C for 2 h. EquiPhi29 conditions

213   were optimized to retain the highest amount of dsDNA based on Povilaitis et al., 2016, the

214   manufacturer's report, and an optimization experiment (Povilaitis et al., 2016) (Supp. 1A).

215   Total DNA (100 ng) and RCA products (100 ng) generated using the TempliPhi

216   Amplification Kit were treated with 1 μL (1 U) of Mung Bean nuclease (New England Biolabs,

217   Ipswich, MA), 3 μL of CutSmart Buffer (New England Biolabs) in a 30 μL reaction volume for

218   30 min at 30°C. The solution was inactivated with 3 μL of SDS (0.01%), and DNA was

219   recovered by ethanol precipitation, according to the manufacturer's specifications. RCA products

220   (11 μL) generated using the TempliPhi Amplification Kit were also treated with 1.0 μL (1 U) of

221   Klenow (large subunit) (New England Biolabs) and 1.0 μL (1 U) of T4 DNA polymerase (New

222   England Biolabs) in a mixture of 5.0 μL 10X NEB Buffer #2 (New England Biolabs), 0.5 μL 10

223   mM dNTP, and 31.5 μL nuclease-free water at 25°C for 1 h. The reaction was inactivated by

224   incubation at 75°C for 1 h. After the repair reaction, residual salt and enzyme were removed by

225   suspending 60 μL of SPRIselect beads (Beckman Coulter, Pasadena CA) in the 50 μL

226   RCA/repair reaction. The mixture was incubated at room temperature for 5 min, placed on a

227   DynaMag^{Tm}-2 magnetic rack (Thermo Fisher Scientific, Waltham MA) for 5 min at room

228   temperature or until the liquid was clear. The liquid was removed and the bead pellet was

229   washed in 200 μL of 80% ethanol on the magnetic rack for 30 sec. The ethanol was removed and

230   air-dried for 5 min on the magnetic rack. The pellet was resuspended in 17 μL of nuclease-free

231   water.

232   The concentrations of the RCA products after the various treatments described above

233   were measured using a Qubit 3.0 fluorometer with the dsDNA HS assay kit or ssDNA assay kit,

234 according to manufacturer's instructions (Thermo Fisher Scientific, Waltham MA). The dsDNA

235 HS assay kit only detects dsDNA, while the ssDNA assay kit detects both ssDNA and dsDNA

236 (i.e. total DNA). For all dsDNA concentration measurements (e.g., Figure 2), Qubit fluorometer

237 readings were used to calculate the amount of DNA. The amount of total dsDNA (in nanograms)

238 was calculated directly using the high sensitivity dsDNA buffer to measure the concentration

239 (ng/μL) and multiplying by the volume of the RCA reaction. Total ssDNA mass was estimated

240 by multiplying the concentration (ng/μL) determined using ssDNA buffer by the volume of the

241 RCA reaction, and subtracting the total mass of dsDNA determined using high sensitivity

242 dsDNA HS assay kit.

243 *2.5. Library Preparation*

244   Total DNA, size-selected DNA, or virion DNA (2 μL) from Kibandameno leaves, tomato

245 leaves, or whiteflies was amplified using EquiPhi29 DNA polymerase as described above. Two

246 separate reactions were set up for each sample. Each RCA reaction was treated with Klenow and

247 T4 DNA polymerases followed by a purification step using SPRIselect beads, as described

248 above. After the clean-up step, each RCA reaction was diluted to 0.2 ng/μL (1 ng total in 5 μL)

249 for library construction. Libraries were prepared using the Nextera XT DNA Library Prep Kit

250 (Illumina, San Diego CA) following manufacturer's instructions using Unique Dual Index

251 adaptors (Integrated DNA Technologies, San Jose CA) and 12 rounds of PCR. The Nextera XT

252 DNA Library Prep Kit was chosen because of its rapid library preparation, low input of DNA,

253 and optimization for small genomes. The libraries were cleaned with 40 μL of SPRIselect beads,

254 as described above. The libraries were analyzed for size distribution (400-800 bp), yield, and

255 quality using a 2100 Bioanalyzer Instrument (Agilent Technologies, Santa Clara, CA). The

256 concentration of each library was determined using a Qubit 3.0 fluorometer using the dsDNA HS

257   assay kit as described above. Libraries were diluted to 15 nM, and equal molar amounts were

258   pooled for sequencing on an Illumina MiSeq platform.

259   The molarity of each library was determined using the following formula:

260   $(ng/\mu L)/(nmol/\mu L) \times (1 \times 10^6)$. The molecular weight of each library was determined by taking

261   the average base-pair length from the Bioanalyzer profile multiplied by the average mass of the

262   four nucleotide bases plus the weight of 5'-PO_4 ((average base-pair length x 607.8) + 157.9).

263   The average mass of nucleotide bases and the MW of 5'-PO_4 was taken from Thermo Fisher

264   Scientific DNA and RNA Molecular Weight and Conversion guide (Scientific). Libraries were

265   pooled for sequencing on an Illumina MiSeq instrument (Fig. 1). A full printable version of our

266   protocol is available at cassavavirusevolution.vcl.ncsu.edu.

267   *2.6. Data Analysis*

268   Raw sequencing data were processed using Cutadapt (v.1.16.3) to remove the universal

269   3' adapters from the paired-end reads and to trim the 5' ends to give fastq quality scores > 30

270   (Martin, 2011). The quality-controlled reads were aligned to the DNA-A and DNA-B

271   components of ACMV and EACMCV or ToMoV using BWA mem (v. 0.8) with default

272   parameters (Li, 2013; Li et al., 2009). Quality-controlled reads were also aligned to the cassava

273   reference genome v.7 (Bredeson et al., 2016) for cassava plant samples, to the tomato reference

274   SL4.0 assembly (Hosmani et al., 2019) for tomato samples, and to MEAM1 assembly (GenBank

275   ASM185493v1) (Chen et al., 2016) for whitefly samples. Duplicate reads were discarded using

276   Picard MarkDuplicates (v. 2.18.2.1, http://broadinstitute.github.io/picard/). Samtools idxstats (v.

277   2.0.3) was used to generate mapping statistics (Li et al., 2009). Sufficient read coverage was

278   designated as 1000X fold coverage (~20,000 reads/genome) based on (Juárez et al., 2019).

279   Coverage was calculated using the following formula from Illumina (coverage=read length X

280   number of reads/genome length). For workflow and full parameters see Galaxy workflow,

281   ViralSeq (cassavavirusevolution.vcl.ncsu.edu) (Giardine et al., 2005). Raw Illumina data are

282   available at the NCBI Sequence Read Archive (PRJNA658475).

3. Results

3.1. Analysis of RCA variability

285   Begomoviruses have circular ssDNA genomes that are converted to dsDNA during viral

286   replication in plants. Viral ssDNA accumulates to high levels during infection, while viral

287   dsDNA occurs at much lower levels. Many library protocols for short-read sequencing involve

288   the ligation of adapters to dsDNA ends or transposase-mediated fragmentation and tagging of

289   dsDNA. Thus, the *in vitro* conversion of viral ssDNA to dsDNA is the first step during library

290   construction for ssDNA viruses. RCA is used frequently to amplify circular viral DNA genomes

291   and to convert viral ssDNA to dsDNA (Inoue-Nagata et al., 2004; Dean et al., 2001). We

292   examined the efficiency of RCA to convert ssDNA to dsDNA and several parameters that might

293   influence the amount of virus-specific dsDNA available for library construction.

294   Total DNA isolated at 28 dpi from four symptomatic Kibaha plants infected with ACMV

295   and EACMCV was incubated in RCA reactions containing phi29 and random hexamers

296   (TempliPhi Amplification Kit). The RCA reactions and an equal amount of unamplified total

297   DNA were digested with Mung Bean nuclease (MB) to remove ssDNA from the samples. RCA

298   increased the amount of total DNA 10-fold relative to input (Fig. 2A). The amounts of the input

299   DNA and the DNA after RCA were both greatly reduced by MB treatment, indicating that most

300   of the DNA before and after RCA is single-stranded and therefore cannot be ligated to library

301   adapters (Fig. 2A).

302   For successful library construction, we sought to increase the amount of viral dsDNA

303   after RCA. During the RCA de-branching step, ssDNA overhangs may be present on dsDNA

304   products, preventing adaptor ligation and leading to exclusion from the final library. To decrease

305   ssDNA overhangs after RCA, we used an end repair reaction to convert ssDNA overhangs to

306   dsDNA. Using the same total DNA sample in Fig. 2A, RCA was performed followed by an end-

307   repair by T4 polymerase and DNA polymerase I (Klenow fragment). The end-repair reaction

308   increased the amount of dsDNA 2-fold (Fig. 2B), indicating that repairing the debranched ends

309   increased the amount of dsDNA. We also tested random primers versus virus-specific primers in

310   the RCA reaction and found that random primers resulted in equal or higher levels of dsDNA

311   depending on the concentration of virus-specific primers, supporting findings by Dean *et al.*,

312   2001 (Supp. 1B).

313   To further increase the amount of dsDNA after RCA, we tested a modified form of phi29

314   DNA polymerase marketed as EquiPhi29, which has been reported to increase dsDNA output up

315   to 7-fold (Povilaitis et al., 2016). Total DNA was amplified in RCA reactions containing the

316   phi29 or the EquiPhi29 DNA polymerase. The amounts of dsDNA and ssDNA were measured

317   using the Qubit dsDNA HS assay kit and ssDNA assay kit as described in the methods. The

318   EquiPhi29 DNA polymerase yielded ~175-fold more ssDNA and 5-fold more dsDNA than the

319   phi29 DNA polymerase (Fig. 2C). Even though most of the increase in RCA products was

320   ssDNA, the 5-fold increase in dsDNA when combined with the 2-fold increase after the DNA

321   end-repair reaction resulted in more dsDNA available for ligation to library adapters.

322   During the process of testing different parameters, we noticed that RCA was highly

323   variable in DNA output. Four total DNA samples (1-4) isolated from symptomatic Kibandameno

324   leaves were amplified using RCA with EquiPhi29 and phi29 (Fig. 2D). This process was

325   repeated twice generating two technical replicates for each sample. The dsDNA concentration of

326   each sample and its technical replicate were measured using a Qubit dsDNA HS assay kit (Fig.

327   2D). Two of the four samples had technical replicates that differed in concentration by more than

328   10-fold (samples 1 and 4, Fig. 2D). Variability was also observed with phi29 (data not shown).

329   This problem was overcome by standardizing the amount the RCA product (2 μL at 5 ng/μL, i.e.

330   10 ng DNA) used for library construction. If the yield of the RCA product from a given reaction

331   was insufficient for dilution to 5 ng/μL, that reaction was repeated.

332   *3.2. Total DNA versus size-selected DNA from leaf tissue*

333   Our goal was to develop a protocol where we could achieve sufficient read coverage to

334   detect viral variants across a complete transmission cycle. Based on the coverage reported by

335   Juárez et al., (2019) to detect viral variants and our calculations, we set 1000X coverage (ca.

336   20,000 150-bp reads/genome component) as our minimum coverage for detecting low viral

337   variants occurring at 3% and 1% frequency in the population (for 30 and 10 variant-supporting

338   reads, respectively). To achieve this goal, we examined additional methods to increase the

339   number of reads mapping to the viral genomes.

340   The DNA-A and DNA-B components of the ACMV and EACMCV genomes are ca. 2.8

341   Kb in size and, as such, are much smaller than plant genomic DNA. Hence, we asked if size

342   selection would increase the number of reads mapping to the viral genomes. We used the

343   BluePippin system to select for DNA < 6 Kb from total DNA samples isolated from

344   symptomatic Kibandameno leaves from two plants. The starting total DNA and the size-selected

345   DNA were amplified using the optimized RCA protocol. Libraries were generated using our

346   experimental pipeline (Fig. 1) and sequenced on the Illumina MiSeq platform. We sequenced

347   two technical replicates for each sample. After processing and mapping the resulting reads to the

348   ACMV and EACMCV reference genomes and the cassava reference, we found that nearly all of

349   the reads mapped to the viral reference genomes when the DNA was size-selected (blue)

350   compared to half of the reads for total DNA (light grey) (Fig. 3A). Generally, the use of size-

351   selected DNA (blue) for library construction increased the number of reads mapping to each of

352   the viral genome components compared to total DNA (grey), improving mapping by ~ 2-fold

353   (Fig. 3B). Nearly all of the reads that did not map to the viral genome components but mapped to

354   the cassava reference genome (Fig. 3A), indicating that size selection is an effective method for

355   separating viral DNA from host DNA. Size-selection was effective in increasing the viral read

356   counts in samples with both high and low levels of CMB genome components (Supp. 2A and B),

357   indicating that size selection can produce reliable results over a 10-fold range. However, the

358   virus titer before RCA does not reflect the resulting coverage and read count after RCA and NGS

359   sequencing (compare Supp. 2A and 3). This result also underscores the variability of RCA (Fig.

360   3C).

361   Size-selection also improved read coverage compared to coverage from total DNA for

362   both cassava (Supp. 3A-D) and whitefly (Supp. 3E-H) samples. The coverage was relatively

363   even across the genomes. Dips in coverage were seen in some profiles at the 3' ends of the

364   convergent transcription units (at the ends of the converging arrows) and in the 5' intergenic

365   regions (at the ends of the linear maps), but the coverage was still above 1000X.

366   After observing that size selection increased viral read count, we evaluated whether

367   virion DNA containing only packaged viral ssDNA would also increase viral read count (Fig.

368   3C). The resulting average read count (yellow) from three bioreplicates was highly variable and

369   500-1000 fold lower than the average read counts of total or size-selected DNA (Fig. 3B).

370   *3.3. Sequencing viral DNA from viruliferous whiteflies*

371   We used the ToMoV-tomato-whitefly pathosystem to assess if our optimized protocols

372   could be applied to another begomovirus. As with the cassava pathosystem, sequencing libraries

373   generated from total DNA (grey) isolated from a ToMoV-infected tomato plant (source plant)

374   resulted in fewer viral reads than libraries constructed from size-selected DNA (blue; Fig. 4A).

375   The average reads from virions for ToMoV DNA-A were similar to total DNA and less than

376   size-selected DNA, while the average read counts from virions for ToMoV DNA-B were lower

377   than total and size-selected DNA (Fig. 4A). This underscores the variability of sequencing from

378   virions. Examining the average percent reads mapping to ToMoV versus host DNA (source

379   plant), we found that over 99% of the reads mapped to ToMoV when using size-selected DNA

380   (Fig. 4B). Using total DNA and virion DNA resulted in ~30% and ~25% of the reads mapping to

381   ToMoV, respectively. This confirms the advantage of size-selection seen in the cassava

382   pathosystem (Fig. 3).

383   We also sequenced DNA from groups of 5 whiteflies that had acquired ToMoV virions

384   from the sampled source plant. We sequenced groups of whiteflies with low, medium, and high

385   viral loads as determined by qPCR. The low, medium and high load groups were split into total

386   DNA and size-selected DNA treatments and sequenced. Read counts for the total DNA samples

387   increased with viral load (Fig. 4C) and were lower than read counts for total DNA from infected

388   tomato (Fig. 4A). In contrast, read counts for size-selected DNA samples (blue) were similar

389   across the different viral load levels and were 20-fold higher than the total whitefly DNA

390   samples (grey; Fig. 4B). Overall, the percent of reads mapping to the viral genome was greater

391   than 90% for size-selected DNA (Fig. 4D). Size-selection also resulted in a 6-fold increase in

392   read coverage compared to total DNA (Supp 3E-H).

393   We also attempted to sequence virion DNA from ToMoV-infected tomato (Fig. 4A) and

394   three sets of five viruliferous whiteflies (Fig. 4E). The resulting reads for virion DNA (yellow)

395   from the ToMoV-infected tomato were variable between the DNA-A and DNA-B components,

396   and the average read count was 100-fold lower than total DNA (grey) and size-selected DNA

397   (blue). The resulting reads from virion DNA (yellow) from viruliferous whiteflies were less than

398   1000X coverage and varied between bioreplicates, indicating that sequencing from whitefly

399   virions was not reproducible. It is also important to note that sequencing total and size-selected

400   DNA provides information both viral ssDNA and dsDNA while sequencing virion DNA only

401   yields sequence data about ssDNA.

402   **4. Discussion**

403   In this study, we examined the impact of RCA reaction conditions and size selection on

404   short-read sequencing of begomovirus DNA. Our optimized protocol effectively enriched for

405   viral DNA and produced short-read sequence data from enhanced RCA reaction products across

406   a range of viral loads. Using size-selected DNA, over 90% of the reads mapped to the viral

407   reference genomes from cassava (Fig. 3A). Without size selection, ca. 50% of the reads mapped

408   to the viral genome and the remaining 50% mapped to the host genome (Fig. 3A). Given that

409   both approaches can yield high numbers of viral reads, using total DNA for library construction

410   may be the preferred approach for plant samples when access to size fractionation

411   instrumentation, cost, and/or time are limiting. A recent study similarly concluded that size

412   selection can be beneficial for long-read sequencing of begomoviruses, which has advantages for

413   certain applications (Mehta et al. 2019).

414   Previous studies using RCA and short-read sequencing to characterize begomovirus

415   sequences reported less than 50% of the reads mapping to the viral genome and even lower

Aimone et al.   20

416   proportions when the RCA step was omitted (Kathurima, 2016). Sequencing of CMBs yielded

417   mapping ranges of 0.87-6.9% from cassava (Kathurima, 2016) and 0.9-29.6% from *Nicotiana*

418   *benthamiana* (Chen et al., 2019). Low read counts following RCA were also observed for tomato

419   leaf curl New Delhi virus (0.47-1.05 %; (Juárez et al., 2019) and euphorbia yellow mosaic virus

420   (1.24-1.35%; (Richter et al., 2016). Our improved sequence method resulted in at least 7X higher

421   viral mapping reads for CMBs and 66X higher than other begomoviruses reported in the

422   literature.

423   Our methods can be used to characterize viral DNA sequences in whiteflies (Fig. 4B).

424   Size selection had a much larger impact on viral read counts from viruliferous whitefly samples

425   compared to infected plant samples, resulting in at least 1000X coverage across a range of viral

426   loads. Sequencing total DNA from whiteflies results in 1000X read coverage when viral loads

427   are high but not when they are low. In contrast, a wide range of viral loads was successfully

428   sequenced using both size selection and total DNA approaches from infected plants. Sequencing

429   viral sequences from whitefly virions produced average viral read counts that were highly

430   variable and 100-fold lower than that average read count from total and size-selected DNA (Fig.

431   4C and E). Currently, most NGS sequencing from whiteflies is from enriched virions for vector-

432   enabled metagenomic surveys (Ng et al., 2011; Rosario et al., 2015). We found that sequencing

433   from virions did not provide enough coverage and read depth for studying virus population

434   diversion in pools of 5 whiteflies.

435   We found that RCA was not efficient at converting ssDNA to dsDNA (Fig. 2A). Even

436   with an improved DNA polymerase (EquiPhi29), most of the RCA product is ssDNA. RCA has

437   a preference to amplify ssDNA as linear, concatenated copies with low conversion of ssDNA to

438   dsDNA, which can be improved by increasing the reaction incubation time to over 25 hours

439   (Ducani, Bernardinelli, and Högberg, 2014; Zhang and Tanner, 2017). However, the Equiphi29

440   DNA polymerase resulted in ~5-fold more dsDNA after RCA with only a 2-hour incubation

441   time, increasing the amount of viral DNA template available for library construction in much

442   shorter reaction time (Fig. 2C). We also found that the amount of DNA produced by RCA varied

443   even when reactions contained the same input DNA (Fig. 2D). Thus, it is important to

444   standardize the amount of RCA product used for library preparation.

445   **6. Conclusion**

446   We established a short-read sequencing protocol for ssDNA viruses that provides high

447   numbers of reads that map to viral reference genomes. The method can use total DNA or size-

448   selected DNA from leaf and whitefly samples that are amplified using random primers and a

449   modified phi29 DNA polymerase prior to library construction. We also found that RCA is

450   variable and is strongly biased towards the amplification of ssDNA products. We cannot fully

451   explain the poor conversion rate to dsDNA, and further studies are needed to understand how

452   ssDNA is converted to dsDNA during RCA. In summary, we have developed an improved tool

453   for begomovirus DNA diagnostics and studying begomovirus population dynamics. Our

454   approach should be applicable to other CRESS DNA viruses.

455   **Author contributions**

456   CDA - Experimental design, execution, and analysis; manuscript preparation

457   JSH - Experimental design and data analysis; manuscript preparation

458   AED - Experimental design, execution, and data analysis; manuscript preparation

459   DOD - Experimental execution

460   IC - Data analysis

461   SD- Experimental design

462   LHB - Experimental design and manuscript preparation

463   **Funding**

466

467   **Declaration of Competing Interest**

468   The authors declare that they have no conflict of interest.

469   **Acknowledgments**

474   **References**

475   Abouzid, A.M., Polston, J.E. and Hiebert, E., 1992. The nucleotide sequence of tomato mottle
476   virus, a new geminivirus isolated from tomatoes in Florida. J Gen Virol 73, 3225-3229.

477   Acevedo, A. and Andino, R., 2014. Library preparation for highly accurate population
478   sequencing of RNA viruses. Nat Protoc 9, 1760-1769.

479   Acevedo, A., Brodsky, L. and Andino, R., 2014. Mutational and fitness landscapes of an RNA
480   virus revealed through population sequencing. Nature 505, 686-90.

481   Ariyo, O.A., Atiri, G.I., Dixon, A.G.O. and Winter, S., 2006. The use of biolistic inoculation of
482   cassava mosaic begomoviruses in screening cassava for resistance to cassava mosaic
483   disease. J of Virol Methods 137, 43-50.

484   Bottcher, B., Unseld, S., Ceulemans, H., Russell, R.B. and Jeske, H., 2004. Geminate structures
485   of African cassava mosaic virus. J Virol 78, 6758-65.

486 Bredeson, J.V., Lyons, J.B., Prochnik, S.E., Wu, G.A., Ha, C.M., Edsinger-Gonzales, E.,
487   Grimwood, J., Schmutz, J., Rabbi, I.Y., Egesi, C., Nauluvula, P., Lebot, V., Ndunguru, J.,
488   Mkamilo, G., Bart, R.S., Setter, T.L., Gleadow, R.M., Kulakow, P., Ferguson, M.E.,
489   Rounsley, S. and Rokhsar, D.S., 2016. Sequencing wild and cultivated cassava and
490   related species reveals extensive interspecific hybridization and genetic diversity. Nature
491   Biotechnol 34, 562-570.

492 Cabrera-Ponce, J., López, L., Assad-Garcia, N., Medina-Arevalo, C., Bailey, A. and Herrera-
493   Estrella, L., 1997. An efficient particle bombardment system for the genetic
494   transformation of asparagus (Asparagus officinalis L.). Plant Cell Rep 16, 255-260.

495 Chen, K., Khatabi, B. and Fondong, V.N., 2019. The AC4 Protein of a Cassava Geminivirus Is
496   Required for Virus Infection. Mol Plant-Microbe Interactions 32, 865-875.

497 Chen, W., Hasegawa, D.K., Kaur, N., Kliot, A., Pinheiro, P.V., Luan, J., Stensmyr, M.C., Zheng,
498   Y., Liu, W., Sun, H., Xu, Y., Luo, Y., Kruse, A., Yang, X., Kontsedalov, S., Lebedev, G.,
499   Fisher, T.W., Nelson, D.R., Hunter, W.B., Brown, J.K., Jander, G., Cilia, M., Douglas,
500   A.E., Ghanim, M., Simmons, A.M., Wintermantel, W.M., Ling, K.-S. and Fei, Z., 2016.
501   The draft genome of whitefly Bemisia tabaci MEAM1, a global crop pest, provides novel
502   insights into virus transmission, host adaptation, and insecticide resistance. BMC Biology
503   14, 110.

504 Chowda Reddy, R.V., Dong, W., Njock, T., Rey, M.E.C. and Fondong, V.N., 2012. Molecular
505   interaction between two cassava geminiviruses exhibiting cross-protection. Virus Res
506   163, 169-177.

507 Claverie, S., Ouattara, A., Hoareau, M., Filloux, D., Varsani, A., Roumagnac, P., Martin, D.P.,
508   Lett, J.-M. and Lefeuvre, P., 2019. Exploring the diversity of Poaceae-infecting
509   mastreviruses on Reunion Island using a viral metagenomics-based approach. Sci Rep 9,
510   12716.

511 de la Iglesia, F. and Elena, S.F., 2007. Fitness Declines in Tobacco Etch
512   Virus upon Serial Bottleneck Transfers. J of Vir 81, 4941.

513 Dean, F.B., Hosono, S., Fang, L., Wu, X., Faruqi, A.F., Bray-Ward, P., Sun, Z., Zong, Q., Du,
514   Y., Du, J., Driscoll, M., Song, W., Kingsmore, S.F., Egholm, M. and Lasken, R.S., 2002.
515   Comprehensive human genome amplification using multiple displacement amplification.
516   Proc Natl Acad Sci U S A 99, 5261-6.

517 Dean, F.B., Nelson, J.R., Giesler, T.L. and Lasken, R.S., 2001. Rapid amplification of plasmid
518   and phage DNA using Phi 29 DNA polymerase and multiply-primed rolling circle
519   amplification. Genome Res 11, 1095-1099.

520 Dickins, B. and Nekrutenko, A., 2009. High-resolution mapping of evolutionary trajectories in a
521   phage. Genome Biol Evol 1, 294-307.

522 Ducani, C., Bernardinelli, G. and Högberg, B., 2014. Rolling circle replication requires single-
523   stranded DNA binding protein to avoid termination and production of double-stranded
524   DNA. Nucleic Acids Res 42, 10596-604.

525 Duffy, S. and Holmes, E.C., 2009. Validation of high rates of nucleotide substitution in
526   geminiviruses: phylogenetic evidence from East African cassava mosaic viruses. J Gen
527   Virol 90, 1539-47.

528 Duffy, S., Shackelton, L. A. & Holmes, E. C., 2008. Rates of evolutionary change in viruses:
529   patterns and determinants. Nat. Rev. Genet 9, 267-276.

530 Elena, S.F., Fraile, A. and García-Arenal, F. 2014. Chapter Three - Evolution and Emergence of
531   Plant Viruses. In: Maramorosch, K. and Murphy, F.A. (Eds), Adv Virus Res, Academic
532   Press, pp. 161-191.

533 Elena, S.F. and Sanjuán, R., 2007. Virus Evolution: Insights from an Experimental Approach.
534   Annu Rev Ecol, Evol, and S 38, 27-52.

535 FAOSTAT, 2016. FAO Statistical Databases. http://faostat.fao.org/ Food and Agriculture
536   Organization (FAO) of the United Nations, Rome, Italy

537 Fondong, V.N. and Chen, K., 2011. Genetic variability of East African cassava mosaic
538   Cameroon virus under field and controlled environment conditions. Virol 413, 275-282.

539   Fondong, V.N., Pita, J.S., Rey, M.E., de Kochko, A., Beachy, R.N. and Fauquet, C.M., 2000.
540   Evidence of synergism between African cassava mosaic virus and a new double-
541   recombinant geminivirus infecting cassava in Cameroon. J Gen Virol 81, 287-97.

542   Giardine, B., Riemer, C., Hardison, R.C., Burhans, R., Elnitski, L., Shah, P., Zhang, Y.,
543   Blankenberg, D., Albert, I., Taylor, J., Miller, W., Kent, W.J. and Nekrutenko, A., 2005.
544   Galaxy: a platform for interactive large-scale genome analysis. Genome Res 15, 1451-5.

545   Hanley-Bowdoin, L., Bejarano, E.R., Robertson, D. and Mansoor, S., 2013. Geminiviruses:
546   masters at redirecting and reprogramming plant processes. Nat Rev Microbiol 11, 777-
547   788.

548   Hosmani, P.S., Flores-Gonzalez, M., van de Geest, H., Maumus, F., Bakker, L.V., Schijlen, E.,
549   van Haarst, J., Cordewener, J., Sanchez-Perez, G., Peters, S., Fei, Z., Giovannoni, J.J.,
550   Mueller, L.A. and Saha, S., 2019. An improved de novo assembly and annotation of the
551   tomato reference genome using single-molecule sequencing, Hi-C proximity ligation and
552   optical maps. bioRxiv, 767764.

553   Hoyer, J.S., Fondong, V.N., Dallas, M.M., Aimone, C.D., Deppong, D.O., Duffy, S. and Hanley-
554   Bowdoin, L., 2020. Deeply sequenced infectious clones of key cassava begomovirus
555   isolates from Cameroon. bioRxiv, 2020.08.10.244335.

556   Idris, A., Al-Saleh, M., Piatek, M.J., Al-Shahwan, I., Ali, S. and Brown, J.K., 2014. Viral
557   metagenomics: analysis of begomoviruses by illumina high-throughput sequencing.
558   Viruses 6, 1219-36.

559   Inoue-Nagata, A.K., Albuquerque, L.C., Rocha, W.B. and Nagata, T., 2004. A simple method for
560   cloning the complete begomovirus genome using the bacteriophage φ29 DNA
561   polymerase. J Virol Methods 116, 209-211.

562   Jeske, H., 2018. Barcoding of Plant Viruses with Circular Single-Stranded DNA Based on
563   Rolling Circle Amplification. Viruses 10.

564   Juárez, M., Rabadán, M.P., Martínez, L.D., Tayahi, M., Grande-Pérez, A. and Gómez, P., 2019.
565   Natural Hosts and Genetic Diversity of the Emerging Tomato Leaf Curl New Delhi Virus
566   in Spain. Front in Microbiol 10.

567   Kathurima, T.M., Ateka, E. M., Nyende, A. B., & Holton, T. A., 2016. The rolling circle
568   amplification and next generation sequencing approaches reveal genome wide diversity
569   of Kenyan cassava mosaic geminivirus. Afr J Biotechnol 15, 2045-2052.

570   Lasken, R.S. and Stockwell, T.B., 2007. Mechanism of chimera formation during the Multiple
571   Displacement Amplification reaction. BMC Biotechnol 7, 19-19.

572   Lefeuvre, P., Harkins, G.W., Lett, J.M., Briddon, R.W., Chase, M.W., Moury, B. and Martin,
573   D.P., 2011. Evolutionary time-scale of the begomoviruses: evidence from integrated
574   sequences in the Nicotiana genome. PLoS One 6, e19193.

575   Lefeuvre, P. and Moriones, E., 2015. Recombination as a motor of host switches and virus
576   emergence: geminiviruses as case studies. Curr Opin Virology 10, 14-19.

577   Legg, J.P., Shirima, R., Tajebe, L.S., Guastella, D., Boniface, S., Jeremiah, S., Nsami, E.,
578   Chikoti, P. and Rapisarda, C., 2014. Biology and management of Bemisia whitefly
579   vectors of cassava virus pandemics in Africa. Pest manag sci.

580   Li, H., 2013. Aligning sequence reads, clone sequences and assembly contigs with BWA-MEM.
581   arXiv, 1303.3997.

582   Li, H., Handsaker, B., Wysoker, A., Fennell, T., Ruan, J., Homer, N., Marth, G., Abecasis, G.,
583   Durbin, R. and Genome Project Data Processing, S., 2009. The Sequence Alignment/Map
584   format and SAMtools. Bioinfo 25, 2078-2079.

585   Lima, A.T.M., Silva, J.C.F., Silva, F.N., Castillo-Urquiza, G.P., Silva, F.F., Seah, Y.M.,
586   Mizubuti, E.S.G., Duffy, S. and Zerbini, F.M., 2017. The diversification of begomovirus
587   populations is predominantly driven by mutational dynamics. Virus evolution 3, vex005.

588 Lou, D.I., Hussmann, J.A., McBee, R.M., Acevedo, A., Andino, R., Press, W.H. and Sawyer,
589   S.L., 2013. High-throughput DNA sequencing errors are reduced by orders of magnitude
590   using circle sequencing. Proc Natl Acad Sci U S A 110, 19872-19877.

591 Martin, M., 2011. Cutadapt removes adapter sequences from high-throughput sequencing reads.
592   2011 17, 3.

593 Mehta, D., Hirsch-Hoffmann, M., Were, M., Patrignani, A., Zaidi, S.S.-E.A., Were, H.,
594   Gruissem, W. and Vanderschuren, H., 2019. A new full-length circular DNA sequencing
595   method for viral-sized genomes reveals that RNAi transgenic plants provoke a shift in
596   geminivirus populations in the field. Nucleic Acids Res 47, e9-e9.

597 Moriones, E. and Navas-Castillo, J., 2000. Tomato yellow leaf curl virus, an emerging virus
598   complex causing epidemics worldwide. Virus Res 71, 123-34.

599 Ndunguru, J., De León, L., Doyle, C.D., Sseruwagi, P., Plata, G., Legg, J.P., Thompson, G.,
600   Tohme, J., Aveling, T., Ascencio-Ibáñez, J.T. and Hanley-Bowdoin, L., 2016. Two Novel
601   DNAs That Enhance Symptoms and Overcome CMD2 Resistance to Cassava Mosaic
602   Disease. J Virol 90, 4160-4173.

603 Ng, T.F.F., Duffy, S., Polston, J.E., Bixby, E., Vallad, G.E. and Breitbart, M., 2011. Exploring
604   the Diversity of Plant DNA Viruses and Their Satellites Using Vector-Enabled
605   Metagenomics on Whiteflies. PLOS ONE 6, e19050.

606 Polston, J.E. and Anderson, P.K., 1997. The Emergence Of Whitefly-Transmitted Geminiviruses
607   in Tomato in the Western Hemisphere. Plant Disease 81, 1358-1369.

608 Povilaitis, T., Alzbutas, G., Sukackaite, R., Siurkus, J. and Skirgaila, R., 2016. In vitro evolution
609   of phi29 DNA polymerase using isothermal compartmentalized self replication
610   technique. Protein engineering, design & selection : PEDS 29, 617-628.

611 Rajabu, C.A., Kennedy, G.G., Ndunguru, J., Ateka, E.M., Tairo, F., Hanley-Bowdoin, L. and
612   Ascencio-Ibáñez, J.T., 2018. Lanai: A small, fast growing tomato variety is an excellent
613   model system for studying geminiviruses. J Virol Methods 256, 89-99.

614   Reyes, M.I., Nash, T.E., Dallas, M.M., Ascencio-Ibáñez, J.T. and Hanley-Bowdoin, L., 2013.

615   Peptide Aptamers That Bind to Geminivirus Replication Proteins Confer a Resistance

616   Phenotype to Tomato Yellow Leaf Curl Virus and Tomato Mottle

617   Virus Infection in Tomato. J Virol 87, 9691-9706.

618   Richter, K.S., Götz, M., Winter, S. and Jeske, H., 2016. The contribution of translesion synthesis

619   polymerases on geminiviral replication. Virology 488, 137-148.

620   Rocha, C.S., Castillo-Urquiza, G.P., Lima, A.T.M., Silva, F.N., Xavier, C.A.D., Hora-Júnior,

621   B.T., Beserra-Júnior, J.E.A., Malta, A.W.O., Martin, D.P., Varsani, A., Alfenas-Zerbini,

622   P., Mizubuti, E.S.G. and Zerbini, F.M., 2013. Brazilian Begomovirus Populations Are

623   Highly Recombinant, Rapidly Evolving, and Segregated Based on Geographical

624   Location. J Virol 87, 5784-5799.

625   Rosario, K., Seah, Y.M., Marr, C., Varsani, A., Kraberger, S., Stainton, D., Moriones, E.,

626   Polston, J.E., Duffy, S. and Breitbart, M., 2015. Vector-Enabled Metagenomic (VEM)

627   Surveys Using Whiteflies (Aleyrodidae) Reveal Novel Begomovirus Species in the New

628   and Old Worlds. Viruses 7, 5553-5570.

629   Ruark-Seward, C.L., Bonville, B., Kennedy, G. and Rasmussen, D.A., 2020. Evolutionary

630   dynamics of Tomato spotted wilt virus within and between

631   alternate plant hosts and thrips. bioRxiv, 2020.01.13.904250.

632   Safari, M. and Roossinck, M.J., 2014. How does the genome structure and lifestyle of a virus

633   affect its population variation? Curr Opin Virol 9, 39-44.

634   Sanjuán, R., Nebot, M.R., Chirico, N., Mansky, L.M. and Belshaw, R., 2010. Viral Mutation

635   Rates. J Virol 84, 9733.

636   Scientific, T.F. DNA and RNA Molecular Weights and Conversions.

637   Sipos, R., Székely, A., Révész, S. and Márialigeti, K. 2010. Addressing PCR Biases in

638   Environmental Microbiology Studies. In: Cummings, S.P. (Ed), Bioremediation:

639   Methods and Protocols, Humana Press, Totowa, NJ, pp. 37-58.

640 Stanley, J. and Gay, M.R., 1983. Nucleotide sequence of of cassava latent virus DNA. Nature
641   301, 2660-2662.

642 Thresh J. M. , D.F.a.G.W.O.-N., 1997. African cassava mosaic disease: the magnitude of the
643   problem. Afr J Root Tuber Crops 2, 13-19.

644 Uzokwe, V.N.E., Mlay, D.P., Masunga, H.R., Kanju, E., Odeh, I.O.A. and Onyeka, J., 2016.
645   Combating viral mosaic disease of cassava in the Lake Zone of Tanzania by
646   intercropping with legumes. Crop Prot 84, 69-80.

647 Wang, X., Li, Y., Ni, T., Xie, X., Zhu, J. and Zheng, Z.M., 2014. Genome sequencing accuracy
648   by RCA-seq versus long PCR template cloning and sequencing in identification of human
649   papillomavirus type 58. Cell biosci 4, 5.

650 Zhang, Y. and Tanner, N.A., 2017. Isothermal Amplification of Long, Discrete DNA Fragments
651   Facilitated by Single-Stranded Binding Protein. Sci Rep 7, 8497.

652 Zhao, L., Rosario, K., Breitbart, M. and Duffy, S. 2019. Chapter Three - Eukaryotic Circular
653   Rep-Encoding Single-Stranded DNA (CRESS DNA) Viruses: Ubiquitous Viruses With
654   Small Genomes and a Diverse Host Range. In: Kielian, M., Mettenleiter, T.C. and
655   Roossinck, M.J. (Eds), Adv Virus Res, AP, pp. 71-133.

656

657 **Table 1.** qPCR Primer Sequences

Primers	Sequence	qPCR target
P3P-AA2F	TCTGCAATCCAGGACCTACC	ACMV DNA-A
P3P-AA2R+4R	GGCTCGCTTCTTGAATTGTC	ACMV DNA-A
ACMVBdiv4	ATTGAGCACCAGGCGATAT	ACMV DNA-B
ACMVBfor1	CACATAGAGGCAGTAGCCATAAA	ACMV DNA-B
EACMVQ1	GTACCATGCGTCGTTTGAATA	EACMCV DNA-A
EACMVQ2	GCAAGTCCCAGAGGAAATAGA	EACMCV DNA-A
EACMVBREV4	GCATCGACTGTGATCGCATAC	EACMCV DNA-B
EACMVBfor1.2	CCAAGGGATACACAAAGATTGC	EACMCV DNA-B
ToMoVA6F	TCAGGTTGTGGTTGAACCGT	ToMoV DNA-A
ToMoVA6R	TTAGACTGTGCGGGACATGG	ToMoV DNA-A
ToMoVB4F	CGACGAGCTATTTGGTGCA	ToMoV DNA-B
ToMoVB4R	TCTCAACTGAGAGCACTCGC	ToMoV DNA-B

658

659

660 **Figure Legends**

661 *Fig 1. Workflow of viral DNA sequencing for short-read sequencing platforms*

662 *Fig 2. Improvements to RCA reactions*

663 (A) The amount of total DNA (-RCA) and total DNA amplified with RCA (+RCA) treated

664 (+MB) or not treated (-MB) with Mung Bean nuclease (MB). (B) The amount of DNA (ng) in an

665 RCA reaction before -end repair and after +end repair. (C) Amount of ssDNA and dsDNA after

666 RCA amplification of total DNA with either Phi29 or EquiPhi29 DNA polymerases. (D) The

667 concentration of the total DNA of technical replicates from 4 cassava leaf DNA samples

668 amplified using RCA.

669 *Fig 3. Size selection increases viral DNA read counts for cassava samples.*

670 (A) The average percent reads mapping to viral DNA (ACMV and EACMCV) and host DNA,

671 and unmapped reads for total DNA (grey) and size-selected DNA (blue) samples. (B) The

672 average number of reads corresponding to ACMV DNA-A (Hosmani et al.), ACMV DNA-B

673 (AB), EACMCV DNA-A (EA), and EACMCV DNA-B for total (grey) and size-selected (blue)

674 DNA samples. (C) The average number of reads corresponding to ACMV DNA-A (Hosmani et

675 al.), ACMV DNA-B (AB) for virion DNA (yellow). The bars in A, B correspond to 2 standard

676 errors from two bio-samples and two technical reps each. The bars in C correspond to 2 standard

677 errors from three bio-samples with two technical replicates each. The asterisks indicate a

678 significant difference (P-value < 0.05) between the viral read counts in size-selected and total

679 DNA in Student's t-tests.

680 *Fig 4. Size selection increases viral DNA read counts for tomato and whitefly samples.*

681 A) The average number of reads corresponding to ToMoV DNA-A (TA) and ToMoV DNA-B

682 (TB) for total (grey), size selected (blue), virion (yellow) DNA samples from the tomato source

683 plant. (B) The average percent reads mapping to viral DNA (ToMoV) and host DNA for total

684 DNA (grey), size-selected DNA (blue), and virion DNA (yellow) samples. (C) The average

685 number of reads corresponding to ToMoV DNA-A (TA) and ToMoV DNA-B (TB) for total

686 (grey) and size-selected (blue) DNA samples from pools of 5 whiteflies with low (30,000-40,000

687 DNA-A copies/ng total DNA), medium (45,000-60,000 DNA-A copies/ng total DNA), and high

688 viral loads (150,000-200,000 DNA-A copies/ng total DNA) virus loads. (D) The average percent

689 reads mapping to viral DNA (ToMoV), host DNA, and whitefly DNA for total DNA (grey), size-

690 selected DNA (blue), and virion DNA (yellow) samples. (E) The average number of reads

691 corresponding to ToMoV DNA-A (TA) and ToMoV DNA-B (TB) for virion DNA (yellow). The

692 bars in A and C correspond to 2 standard errors for three bio-samples with two technical

693 replicates. The asterisks indicate a significant difference (P-value < 0.05) between the viral read

694 counts in size-selected and total DNA in Student's t-tests.

695 *Supp 1. Optimization of RCA conditions*

696 (A) Amount of ssDNA and dsDNA after RCA amplification of total DNA with EquiPhi29

697 polymerase for 2 h and 3 h at 40°C. (B) Amount of dsDNA after RCA amplified with random

698 hexamers (hx) alone or combined with different amounts of virus-specific primers (vs).

699 *Supp 2. Virus levels and virus-mapping read count for cassava biological replicates.*

700 (A) Log viral copy number of ACMV-A (AA0, ACMV-B (AB), EACMCV-A (EA), and

701 EACMCV-B (Bernardo et al.) for biological replicate 1 (green) and biological replicate 2 (blue).

702 (B) Average read count of two technical replicates for biological replicate 1 (green) and 2 (blue)

703 for ACMV-A (Hosmani et al.), ACMV-B (AB), EACMCV-A (EA), and EACMCV-B (Bernardo

704 et al.) without size-selection. (C) Average read count of two technical replicates for biological

705   replicate 1 (green) and 2 (blue) for ACMV-A (Hosmani et al.), ACMV-B (AB), EACMCV-A

706   (EA), and EACMCV-B (Bernardo et al.) with size-selection.

707   *Supp 3. Plots of Illumina read depth across virus segments.*

708   Each row corresponds to one library, from leaf tissue from a cassava plant (A to D) or a single

709   pool of whiteflies (E to H). Pairs of rows correspond to technical duplicate libraries made from

710   total DNA (A and B, E and F) or to size-selected DNA (C and D, G and H). Canonical virus

711   genes are drawn as gray arrows below each set of graphs, left to right for virus sense (AV1, AV2

712   [for ACMV and EACMCV], BV1), and right to left for complementary sense (AC1 to AC4,

713   BC1).

714

Figure 1 Aimone et al

1 RCA with EqiPhi29
Input: 2 µL of total DNA
Time: 2 h at 40°C

2 End Repair Reaction
Input: 11 µL of RCA Reaction
Reagents: Klenow and T4 DNA Pol
Time: 1 h at 25°C

3 Clean Up
Input: 20 µL of end-repaired RCA reaction
Reagents: 1.2X (volume/volume) SPRI select beads

4 Library Prep
Input: 1 ng of cleaned RCA product
Kit: Nextera XT (Illumina)
12 cycles PCR
IDT Unique Dual Indexes

5 Clean Up
Input: 30 µL of library
Reagents: 1.2X (volume/volume) SPRI select bead

6 Pool Libraries
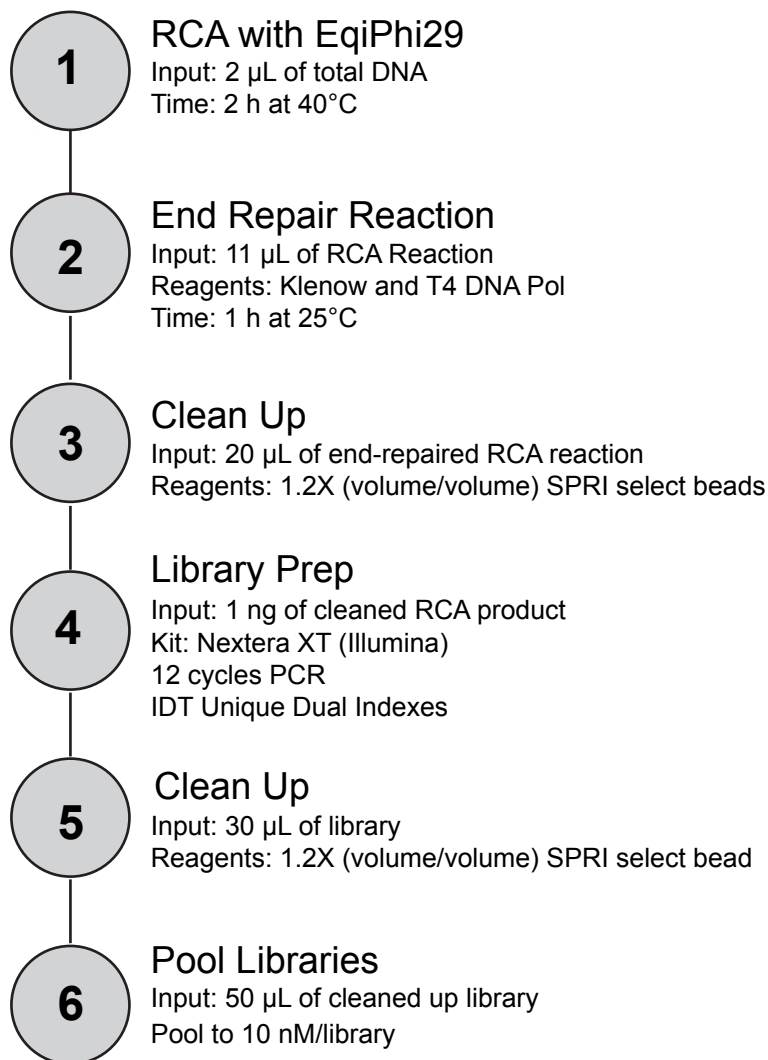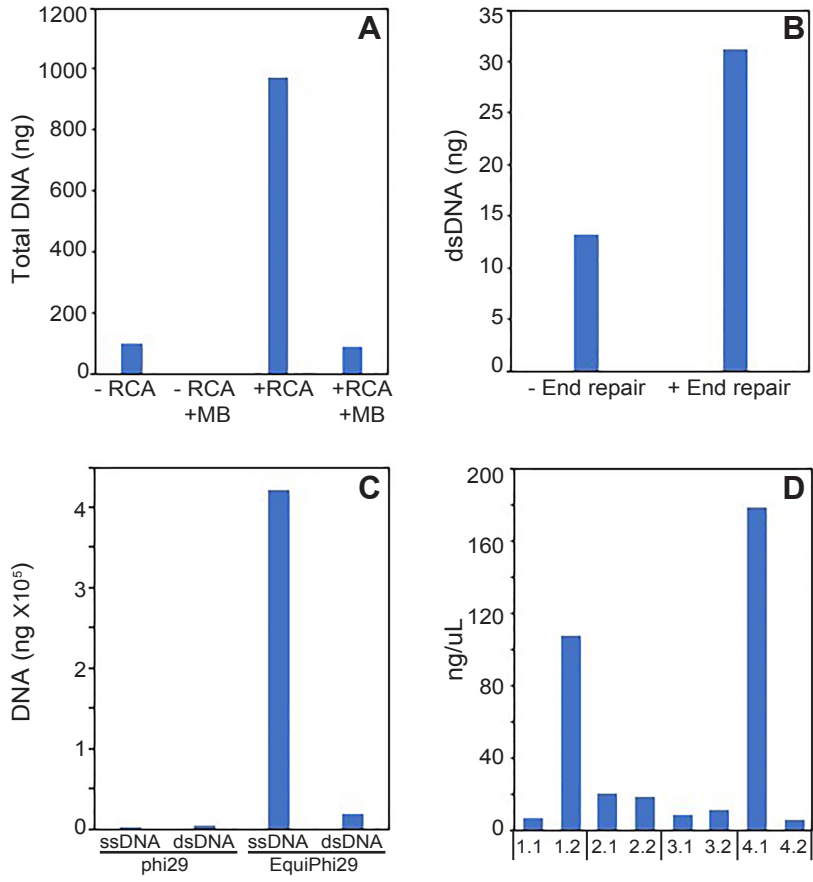Input: 50 µL of cleaned up library
Pool to 10 nM/library

Figure 2 Aimone et al

Figure 3 Aimone et al

Figure 4 Aimone et al